Interference stabilization of molecules with respect to photodissociation by a strong laser field

M. E. Sukharev[1,*] and M. V. Fedorov[2,†]
[1]*Fiber Optics Research Center at the General Physics Institute, Russian Academy of Sciences, 38 Vavilov Street, Moscow, 117942, Russia*
[2]*General Physics Institute, Russian Academy of Sciences, 38 Vavilov Street, Moscow, 117942, Russia*
(Received 10 September 2001; published 27 February 2002)

The ideas of interference stabilization of Rydberg atoms are adapted to photodissociation and stabilization of molecules by a strong laser field. Multiple strong-field-induced Raman-type transitions between vibrational levels of the ground electronic state are taken into account. For the molecular ion H_2^+ matrix elements of these transitions are calculated numerically and the arising equations for probability amplitudes to find a molecule at ground-state vibrational levels are solved (a) in stationary and (b) in the initial-value-problem formulations. In the stationary formulation, complex quasienergies and quasienergy zones are found. Specific values of the light frequency ω are found at which some quasienergy zones narrow with growing light intensity. Such an effect indicates a possibility of stabilization, which is confirmed to occur by a direct solution of the initial-value problem. The calculated total probability of photodissociation per pulse in the dependence on the light peak intensity is shown to decrease its growth with growing light intensity. Dynamics of photodissociation in the stabilization regime and structure of the arising vibrational wave packets are investigated and discussed. The method of description, in which Raman-type vibrational-vibrational transitions are taken into account is compared with that based on the ideas of the field-induced avoided crossing.

DOI: 10.1103/PhysRevA.65.033419 PACS number(s): 42.50.Hz, 32.80.Rm

I. INTRODUCTION

As it is well known [1,2], interference stabilization of Rydberg atoms, photoionized by a strong light field, arises owing to Raman-type (or Λ-type) transitions between Rydberg levels. These transitions provide coherent repopulation of Rydberg levels, subsequent transitions from which to the continuum can interfere with each other and suppress photoionization. The effect was rather widely investigated theoretically, and some of existing experiments on the strong-field stabilization of atoms [3] can be considered as a confirmation of the model of interference stabilization.

In a theoretical study, many interesting features of the phenomenon were discovered. One of them concerns structure of quasienergy levels in dependence on the light intensity I. In the range of intensities $I<I_{cr}\sim\omega^{10/3}$ (where ω is the light frequency and both ω and I are in atomic units) Rydberg levels broaden owing to ionization but broadening remains smaller than spacing between levels, and there is no stabilization. At $I\sim I_{cr}$ broadened levels overlap with each other and form a kind of a quasicontinuum. In the range of higher intensities $I>I_{cr}$ quasienergy levels appear to be narrowing with growing I, and narrowing quasienergy (or dressed-atom) levels appear to be located exactly between neighboring field-free Rydberg levels. Narrowing of quesienergy levels in the strong-field limit is connected directly with the effect of interference stabilization.

In principle, probably, a similar phenomenon (stabilization with respect to photoionization) can occur in molecules excited initially to high (Rydberg) electronic states. As far as we know, such an effect has never been either discussed theoretically or observed experimentally. But its consideration is not the goal of this paper either. Here we will discuss a possibility of a related but different phenomenon. The idea is to look for a possibility of interference stabilization at vibrational levels of a molecule with respect to its photodissociation rather than photoionization. The physics of such a phenomenon can be close to that described above. It is assumed again that in the process of strong-field photodissociation vibrational levels of the molecular ground electronic state can be efficiently repopulated via Raman- or Λ-type transitions (Fig. 1) and subsequent transitions from these levels to an excited unstable electronic state can interfere with and partially cancel each other giving rise to stabilization of a molecule with respect to its photodissociation.

Though the formulated analogy between atomic Rydberg levels and molecular vibrational levels looks quite natural and straightforward, realizability of the described stabilization effect in molecules is far from being evident. The reason is in a great difference in structures of the continua in atoms and molecules and in the resulting difference in dipole matrix elements of bound-free atomic and molecular transitions. Because of these differences many approximations often used and rather well justified in the case of atoms, appear to be absolutely invalid in the case of molecular transitions. Some approximations of this kind discussed below are the flat-continuum approximation, a procedure of adiabatic elimination of the continuum, approximation of almost identical values of all the components of the ionization-width tensor in the case of Rydberg atoms, etc. All of these approximations or their analogs do not work in the case of molecules. For this reason, the molecular problem is much more complicated than the atomic one and hardly can be solved analytically, even approximately. In this paper, for a molecular ion H_2^+, we calculate numerically all the arising matrix elements: dipole bound-free matrix elements and

*Electronic address: maxtheor@fo.gpi.ru
†Electronic address: fedorov@gon.ran.gpi.ru

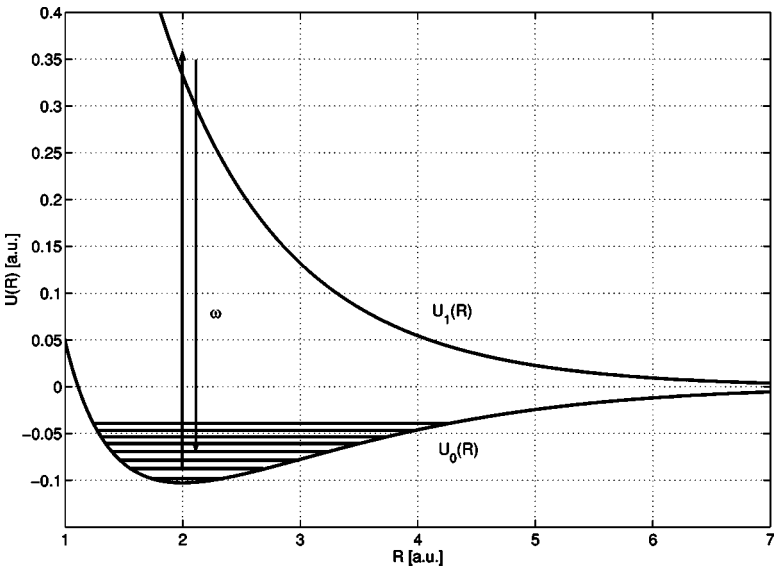

FIG. 1. A scheme of potential curves $U_0(R)$ and $U_1(R)$ for the hydrogen molecular ion H_2^+ (inset) and scheme of Raman- $(\Lambda-)$ type transitions between vibrational levels E_v.

complex matrix elements of Raman-type transitions between vibrational levels of the ground electronic state. The results of such calculations are used to justify the procedure of semiadiabatic elimination of the continuum introduced below. We solve numerically equations for the probability amplitudes to find a molecule at vibrational levels of the ground electronic state. As a result, we find complex quasienergies of a molecule and solutions of the initial-value problem. The results are used to find conditions under which interference stabilization at molecular vibrational levels can occur and to analyze the physics of stabilization.

It should be noted that strong-field stabilization of molecules with respect to their photoionization has been discussed earlier [4–7]. The methods of theoretical analysis were based either on a direct numerical solution of the Schrödinger equation or on the effect known as the field-induced avoided crossing [8]. This method and that based on taking into account multiple Raman-type transitions (used in this paper) are compared briefly below in Sec. V. Our method is applied to molecules, we do believe, it gives an interesting insight into the physics of stabilization in molecules. Besides, in our calculations we consider the case of frequencies, sufficiently high to provide one-photon transitions from low-energy vibrational states of the ground electronic states to the continuum of the first unstable electronic state. As far as we know, such a case has never been considered in earlier works. It is interesting enough that interference stabilization is shown to exist even at low-vibrational levels where analogy with atomic Rydberg levels is minimal.

II. EQUATIONS

Let us consider two lowest-energy bound (U_0) and unstable (U_1) molecular electronic states (respectively, $1\sigma_g$ and $1\sigma_u$ states in the H_2^+ molecule, Fig. 1). Let the light frequency ω be more or less close to the energy of a transition between these two electronic states at the equilibrium distance between nuclei $R=R_e\approx 2$ (if not indicated differently, atomic units are used throughout the paper). Let any other electronic states be out of resonances and transitions to and via them be ignored. At last, let us use the approximation of frozen angular variables of a molecule, which is quite reasonable in the case of short laser pulses (tens femtoseconds) to be considered below. Under these assumptions an expansion of the field-driven molecular wave function in a series of the field-free eigenfunctions can be written in the form

$$\Psi=\psi_0\sum_v C_v(t)\exp(-iE_vt)\varphi_v(R) + \psi_1\int dE\exp(-iEt)C_E(t)\varphi_E(R), \qquad (2.1)$$

where $\psi_{0,1}$ are the electronic wave functions of the ground and first excited electronic states of a molecule, $\varphi_v(R)$ are the vibrational wave functions of the ground electronic state, and $\varphi_E(R)$ are the nuclear wave functions of the unstable electronic state. Equations for the time-dependent probability amplitudes $C_{v,E}(t)$, following from the Schrödinger equation, in the rotating-wave approximation are given by

$$i\dot{C}_v(t)=-\frac{\varepsilon_0(t)}{2}\int dE\exp[i(E_v+\omega-E)t]d_{vE}C_E(t),$$

and

$$i\dot{C}_E(t)=-\frac{\varepsilon_0(t)}{2}\sum_v d_{Ev}\exp[-i(E_v+\omega-E)t]C_v(t), \qquad (2.2)$$

where $\varepsilon_0(t)$ is the pulse field-strength envelope and d_{vE} and d_{Ev} are the dipole matrix elements

$$d_{vE}=\langle\varphi_v|d_{01}(R)|\varphi_E\rangle=(d_{Ev})^* \qquad (2.3)$$

with $d_{01}(R)=\langle\psi_0|d|\psi_1\rangle$.

Equations (2.2) are written for molecules aligned along the field polarization (in the approximation of frozen rota-

tions). This is the case under consideration in this paper. For an ensemble of molecules randomly distributed over θ, ε_0 in Eq. (2.2) must be substituted by $\varepsilon_0 \cos\theta$, where θ is the angle between the molecular axis and polarization, and the results of calculations (e.g., probability of dissociation) must be averaged over θ.

The second of Eqs. (2.2) can be formally integrated and substituted to the first ones to reduce the latter to the form of a set of integrodifferential equations for the functions $C_v(t)$ only

$$\dot{C}_v(t) = -\frac{\varepsilon_0(t)}{4}\int_{-\infty}^{0} dt' \varepsilon_0(t+t') \sum_{v'} C_{v'}(t+t') \times \exp[i(E_v - E_{v'})t] R_{v,v'}(t') \times \exp[-i(E_{v'}+\omega)t'], \tag{2.4}$$

where the kernel functions $R_{v,v'}(\tau)$ are given by

$$R_{v,v'}(t') = \int_0^\infty dE\, d_{vE} d_{Ev'} \exp(iEt'). \tag{2.5}$$

The above-mentioned flat-continuum approximation and adiabatic elimination procedure correspond, respectively, to very slow dependence of the dipole matrix elements d_{vE} on the energy in the continuum E and to the approximation of the kernel functions $R_{v,v'}(\tau)$ by the δ function, $R_{v,v'}(\tau) \propto \delta(\tau)$. As it follows from our direct calculations (see Sec. IV below) none of these approximations is valid in the case of molecules: the dependence of d_{vE} on E is not slow and the functions $R_{v,v'}(\tau)$ are not narrow enough to be approximated by the δ function. Nevertheless, as is shown below, a kind of a semiadiabatic elimination procedure can be formulated and used. The functions $R_{v,v'}(\tau)$ will be shown to be localized near $\tau = 0$ in a region which is small compared to typical variation scales of $C_v(t+\tau)$ and $\varepsilon_0(t+\tau)$ but not compared to $1/\omega$. This means that the functions $C_v(t+\tau)$ and $\varepsilon_0(t+\tau)$ can be substituted by $C_v(t)$ and $\varepsilon_0(t)$ and taken out of the integral on the right-hand side of Eqs. (2.4) to reduce Eqs. (2.4) to simple first-order differential equations

$$\dot{C}_v(t) = -\frac{\varepsilon_0^2(t)}{4}\sum_{v'} C_{v'}(t)\, Q_{v,v'}(\omega) \exp[(E_v - E_{v'})t], \tag{2.6}$$

where $Q_{v,v'}(\omega)$ are the Raman-type matrix elements

$$Q_{v,v'}(\omega) = \int_{-\infty}^{0} d\tau R_{v,v'}(\tau) \exp[-i(\omega + E_{v'})\tau]. \tag{2.7}$$

For H_2^+ the known data about potential curves $U_{0,1}(R)$ [9] and electronic functions $\psi_{0,1}$ [10] were used to calculate numerically field-free nuclear eigenfunctions $\varphi_v(R)$ and $\varphi_E(R)$, the R-dependent electronic-transition dipole moment $d_{01}(R)$, its matrix elements d_{vE} (2.3), kernel functions $R_{v,v'}(\tau)$ (2.5) of the integrodifferential Eqs. (2.4), and Raman-type matrix elements $Q_{v,v'}(\omega)$ (2.7). Then, Eqs. (2.6) were used to solve the initial-value problem and to find the time-dependent probability amplitudes $C_v(t)$. The time-dependent probability of dissociation $w_D(t)$ was determined as

$$w_D(t) = 1 - \sum_v |C_v(t)|^2. \tag{2.8}$$

For Gaussian-like pulses the total probability of dissociation per pulse is given by $w_{D\,tot} = w_D(\infty)$. For pulses ending at finite time τ, $w_{D\,tot} \equiv w_D(\tau)$. Below, $w_D(t)$ (2.8) and $w_{D\,tot}$ are compared with the probability of dissociation determined by the first-order Fermi-Golden-Rule (FGR) formula, integrated over time and raised to the exponent

$$w_D^{\mathrm{FGR}}(t) = 1 - \exp\left(-\frac{\pi}{2}|d_{vE}|^2 \Big|_{E=E_v+\omega} \int_{-\infty}^{t} \varepsilon_0^2(t')dt' \right) \tag{2.9}$$

and $w_{D\,tot}^{\mathrm{FGR}} = w_D^{\mathrm{FGR}}(\tau)$ (for pulses ending at finite time $t = \tau$). It should be emphasized that, though expression (2.9) is more general than the first-order perturbation-theory formula, it corresponds to the approximation of bound-free transitions from a single isolated vibrational level E_v with Raman-type transitions $E_v \rightarrow \text{continuum} \rightarrow E_{v'}$ completely ignored. Coincidence or difference of $w_D^{\mathrm{FGR}}(t)$ and $w_{D\,tot}^{\mathrm{FGR}}$ with $w_D(t)$ and $w_{D\,tot}$ indicate applicability or inapplicability of this approximation.

A substitution $C_v(t) = a_v(t)\exp(iE_v t)$ reduces Eqs. (2.6) to the form

$$\dot{a}_v(t) + iE_v\, a_v(t) = -\frac{\varepsilon_0^2(t)}{4}\sum_{v'} Q_{v,v'}(\omega) a_{v'}(t). \tag{2.10}$$

In the limit of a very smooth pulse envelope $\varepsilon_0(t) \approx \text{const.} = \varepsilon_0$ the coefficients of Eqs. (2.10) do not depend on time, and such equations have stationary, or quasienergy, solutions $a_v(t) = b_v \exp(-i\gamma t)$, where $b_v = \text{const.}$ and γ denotes complex quasienergies. Complex quasienergies are determined as solutions of the equation

$$\det \left\| (\gamma - E_v)\delta_{v,v'} + i\frac{\varepsilon_0^2}{4} Q_{v,v'} \right\| = 0. \tag{2.11}$$

III. MATHEMATICAL DETAILS

To find numerically field-free nuclear eigenfunctions of a molecule $\varphi_v(R)$ for the ground electronic state $U_0(R)$, we have solved the relevant Sturm-Liouville problem and normalized the arising wave functions by one

$$\int_0^\infty \varphi_v(R)\varphi_{v'}(R)dR = \delta_{v,v'}. \tag{3.1}$$

In our further calculations, we have used the first 15 oscillatory wave functions φ_v of the ground electronic state $U_0(R)$, $0 \leqslant v < 14$.

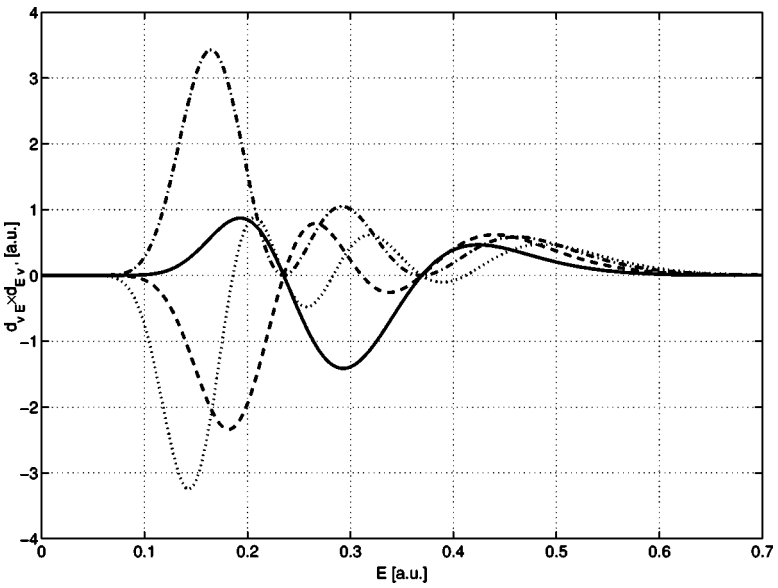

FIG. 2. The product of dipole matrix elements $d_{v,E}\times d_{E,v'}$ vs energy in the continuum E : solid line, $v=2, v'=0$; dashed line, $v=2, v'=1$; dash-dotted line, $v=2, v'=2$; dotted line, $v=2, v'=3$.

To evaluate field-free nuclear wave functions $\varphi_E(R)$ of the first excited electronic state $U_1(R)$, we have solved the boundary problem determined by the nuclear-motion Schrödinger equation

$$\frac{d^2\varphi_E(R)}{dR^2}=2\mu(U_1(R)-E)\varphi_E(R) \tag{3.2}$$

and boundary conditions at small R, which were taken in the form

$$\left.\frac{d\varphi_E(R)}{dR}\right|_{R=R_0}=\beta \quad \text{and} \quad \varphi_E(R_0)=0, \tag{3.3}$$

where μ is the reduced mass of nuclei, $R_0=0.2$ is the minimal internuclear distance at which the potential curve $U_1(R)$ is tabulated [9], $R_0\ll R_e$, $R_e\approx 2$ is the equilibrium internuclear distance for the ground electronic state, and β is a constant, determined by boundary conditions at large R. We have normalized solutions of Eq. (3.2) by the delta-function

$$\int dR\,\varphi_E(R)\varphi_{E'}(R)=\delta(E-E'). \tag{3.4}$$

Such a singular normalization is provided by contribution of a large-R region ($R\gg R_e$), where $\varphi_E(R)$ must have the form [11]

$$\varphi_E(R)\simeq \sqrt[4]{\frac{2\mu}{\pi^2 E}}\cos(kR+\delta) \tag{3.5}$$

with $k=\sqrt{2\mu E}$ and δ being an asymptotic phase . Such an oscillatory dependence on R was found to occur in numerical solutions of Eq. (3.2) at $R\gg R_e$. In accordance with Eq. (3.5), the amplitude of these oscillations must be equal to $\sqrt[4]{2\mu/\pi^2 E}$, and this condition was used to determine the constant β in Eq. (3.3).

As for the second boundary condition in Eq. (3.3), $\varphi_E(R_0)=0$, rigorously, this is the condition to be formulated at $R=0$ rather than R_0. However, as mentioned above, at $R<R_0$ the potential curve $U_1(R)$ is not tabulated and, besides, $R_0\ll R_e$. As at not too high energies E the functions $\varphi_E(R)$ at $R\leqslant R_0$ are very small, a small shift of a position where $\varphi_E(R)=0$ from $R=0$ to $R=R_0$ almost does not change any physical characteristics of a molecule, such as, e.g., dipole matrix elements d_{vE}. We have checked this directly by repeating calculations with the same boundary conditions (3.3) but with twice larger R_0, $R_0=0.4$, and we found that, practically, the results do not change. This proves that the boundary conditions taken in the form (3.3) are sufficiently correct.

The functions $\varphi_E(R)$ were calculated numerically in the energy interval $E\in[10^{-4},1]$ with a step $\delta E=3.3\times 10^{-3}$.

Solutions of the initial-value problem (2.6) with initial conditions $C_v(0)=\delta_{v,v_0}$ were obtained by the Adams-Moulton method with maximum order 12. The pulse envelope was taken in the form

$$\varepsilon_0(t)=\varepsilon_0\sin^2\left(\frac{\pi t}{\tau}\right) \tag{3.6}$$

and, as a rule, the total pulse duration τ was taken to be equal to 70 fs.

IV. RESULTS OF CALCULATIONS

Not dwelling upon further details, let us describe here the main results of calculations carried out in accordance with the outlined program. As a first step we have calculated field-free nuclear eigenfunctions $\varphi_v(R)$ and $\varphi_E(R)$, dipole moment $d_{01}(R)$, and its matrix elements d_{vE} (2.3). The products of dipole matrix elements $d_{v,E}\times d_{E,v}$, for $v=2$ and $v'=0,1,2,3$ are plotted in their dependence on the final-state energy E in Fig. 2. These functions are seen to oscillate, and these oscillations reflect mainly a structure of the ground electronic state vibrational wave functions $\varphi_v(R)$. This struc-

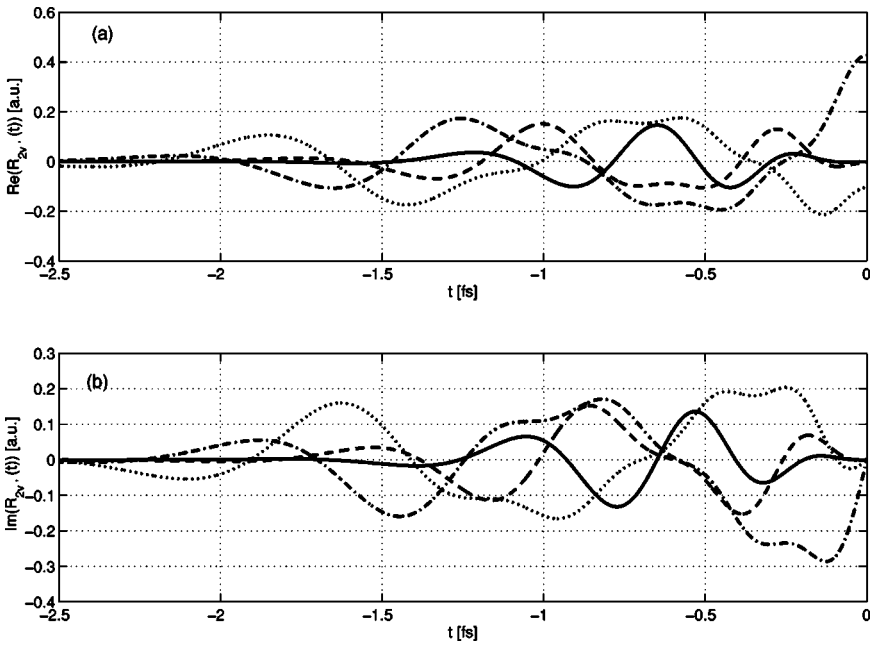

FIG. 3. Real (a) and imaginary (b) parts of the Kernel functions $R_{2,v'}(\tau)$ (2.4): solid line, $v'=0$; dashed line, $v'=1$; dash-dotted line, $v'=2$; dotted line, $v'=3$.

ture manifests itself in the dependencies of d_{vE} on E because the molecular nuclear-motion continuum is not flat: it has a rather sharp border at $E=U_1(R)$. In accordance with the Franck-Condon principle, bound-continuum nuclear transitions are most efficient when a value of the internuclear distance R found from the equation $E=U_1(R)$ is close to those, at which the bound-electronic state nuclear wave functions $\varphi_v(R)$ have their peaks, and this explains the oscillating dependencies of d_{vE} on E.

The next step consists of calculating the kernel functions $R_{v,v'}(\tau)$ (2.5) of the integro-differential Eqs. (2.4). Real and imaginary parts of four functions $R_{2,v}(\tau)$ with $v=0,1,2$, and 3 are plotted in Fig. 3. The functions $R_{v,v'}(\tau)$ are seen to be localized in an interval $\Delta\tau\sim 1.5$ fs around $\tau=0$. For pulses much longer than 1.5 fs their envelope $\varepsilon_0(t+\tau)$ in Eq. (2.4) varies much slower than $R_{v,v'}(\tau)$ and can be approximated by $\varepsilon_0(t)$ and taken out of the integral over τ. The same is true for probability amplitudes $C_{v'}(t+\tau)$ in Eq. (2.4), if only oscillation periods of the functions $C_{v'}(t)$ are much longer than 1.5 fs (and this must be checked *a posteriori*). The described features of the kernel functions $R_{v,v'}(\tau)$ justify transition from the integrodifferential Eqs. (2.4) to the differential ones (2.6) or the semiadiabatic elimination of the continuum. In this approximation, interaction between the ground and excited (unstable) electronic states $U_0(R)$ and $U_1(R)$ is characterized only and completely by the Raman-type two-photon dipole matrix elements $Q_{v,v'}(\omega)$ (2.7) on the right-hand side of Eqs. (2.6). These matrix elements were calculated numerically. For some values of the vibrational quantum numbers v and v' ($v=2$ and $v'=0,1,2$, and 3) the

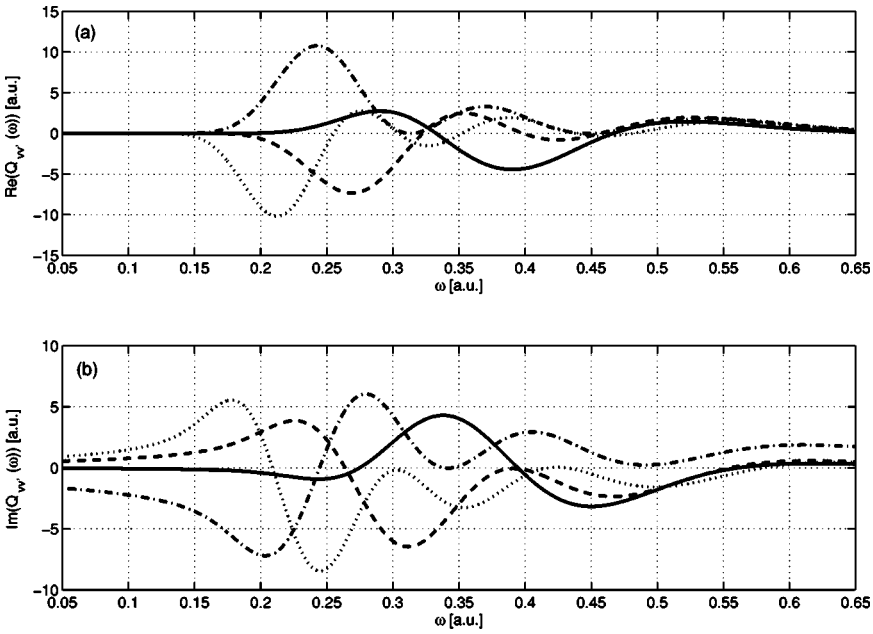

FIG. 4. Real (a) and imaginary (b) parts of Raman-type two-photon matrix elements $Q_{v,v'}(\omega)$: solid line, $Q_{2,0}$; dashed line, $-Q_{2,1}$; dash-dotted line, $Q_{2,2}$; dotted line, $Q_{2,3}$.

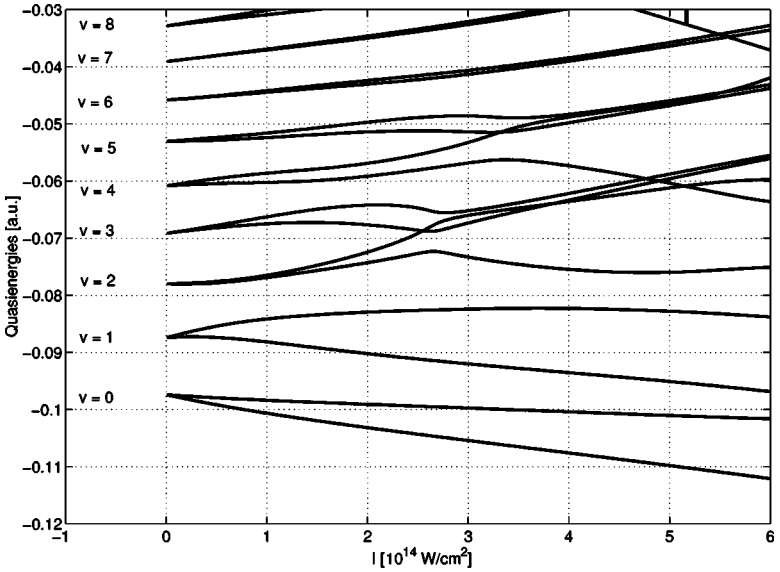

FIG. 5. Quasienergy zones $v=0\cdots8$ at $\omega=0.338$.

results of calculations are shown in Fig. 4.

As it is seen from these results, the Raman-type matrix elements $Q_{v,v'}(\omega)$ are characterized by a rather strong frequency dependence: they oscillate and, as a whole, they are localized in a rather limited range of frequencies ω, outside of which they are small. This last feature indicates a rather well-pronounced resonance character of laser-molecule interaction even in the case of interaction between discrete vibrational levels E_v and the continuous spectrum of the unstable electronic state $U_1(R)$. Also, the Raman-type matrix elements $Q_{v,v'}$ depend strongly on v and v' and they cannot be assumed to be v and v' independent, even approximately. Finally, real and imaginary parts of $Q_{v,v'}$ are found to be, typically, of the same order of magnitude. All of these features of $Q_{v,v'}$ differ from the molecular Raman-type matrix elements from those of Rydberg atoms, which can be approximated often by some constants, almost independent of frequency and quantum numbers [2].

As mentioned above, having found the Raman-type matrix elements $Q_{v,v'}(\omega)$ we can solve both the eigenvalue and initial-value problems [Eqs. (2.11) and (2.6), respectively]. Equation (2.11) determines complex quasienergies of a field-driven molecule. A typical example of calculations is shown in Fig. 5. The upper and lower borders of the quasienergy zones are determined as $\mathrm{Re}(\gamma_v)+\frac{1}{2}|\mathrm{Im}(\gamma_v)|$ and $\mathrm{Re}(\gamma_v)-\frac{1}{2}|\mathrm{Im}(\gamma_v)|$, and γ_v are the solutions of Eq. (2.11) (complex quasienergies). Complex quasienergies and quasienergy zones are calculated in their dependence on the light intensity I at a given frequency ω. The results of Fig. 5 (as well as of Figs. 5–7 and 10–13 below) correspond to $\omega=0.338$. The reason for choosing this specific frequency is explained below. As it is seen from Fig. 5, most of the quasienergy levels (zones) broaden monotonously with a growing light intensity, and this corresponds to faster and faster decay of the corresponding quasienergy states. However, some quasienergy zones in some ranges of intensity demonstrate a rather unusual behavior. In the case of Fig. 5, the quasienergy zones with $v=2$ and $v=3$ at first broaden, then overlap with each

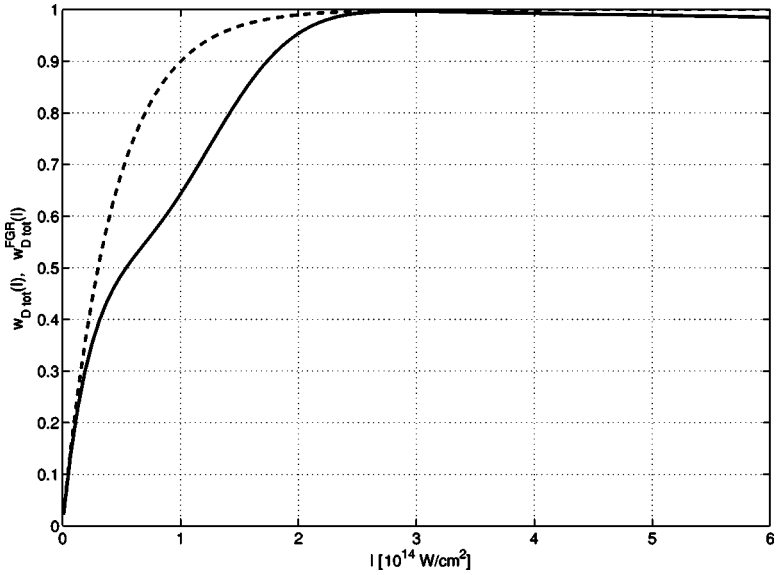

FIG. 6. Exact (2.8) and Fermi-Golden-Rule (2.9) probability of dissociation per pulse (solid and dashed lines) vs the peak light intensity I; $\omega=0.338$, $\tau=70$ fs, and $v_0=2$.

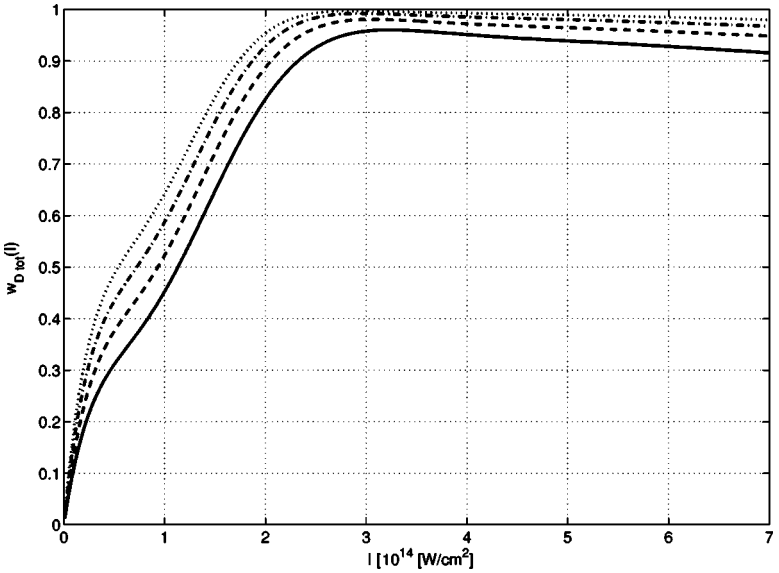

FIG. 7. Total probability of dissociation per pulse $w_{D\,tot}$ vs the peak light intensity I at different values of the pulse duration τ: solid line, $\tau=40$ fs; dashed line, $\tau=50$ fs; dash-dotted line, $\tau=60$ fs; dotted line, $\tau=70$ fs.

other, and at higher intensity ($\gtrsim 2.5\times10^{14}$ W/cm^2) form a very specific structure of a narrow zone at the background of a broad one. The narrow zone itself, at first, slightly broadens and then becomes further narrowing with a growing light intensity. At slightly higher intensities ($\gtrsim 3.3\times10^{14}$ W/cm^2) similar effects occur for a couple of quasienergy zones $v=4$ and $v=5$. The described behavior of quasienergy zones is very similar to that occurring in a two-level model of interference stabilization of Rydberg atoms [2]. However, in the case of molecules, such a two-level-like behavior of quasienergy zones is determined by interaction of many vibrational levels. The picture was checked to change drastically when only two terms (e.g., with $v=2$ and $v=3$) where retained in the sum over v of the expansion (2.1).

Formation of narrow quasienergy zones and their further narrowing with a growing light intesity indicate clearly a possibility of stabilization of a molecule: population at narrow-width quasienergy levels remains bound for longer times than expected from predictions of the generalized Fermi-Golden-Rule formula (2.9). To see the effect of stabilization explicitly, we have to turn to the initial-value problem and its solutions.

The first result of such a solution shown in Fig. 6 is the dependence of the total probability of dissociation per pulse on the peak light intensity I (calculated for $v_0=2$ and at $\tau=70$ fs). The function $w_{D\,tot}(I)$ is plotted together with $w_{D\,tot}^{\mathrm{FGR}}(I)$ (2.9). The curve $w_{D\,tot}(I)$ is seen to have a well-pronounced knee structure, which differs rather strongly $w_{D\,tot}(I)$ from $w_{D\,tot}^{\mathrm{FGR}}(I)$. This difference indicates an importance of the Raman-type transitions $E_v\rightarrow$continuum$\rightarrow E_{v'}$ and can be interpreted as a partial stabilization of a molecule by a strong light field. The difference between $w_{D\,tot}(I)$ and $w_{D\,tot}^{\mathrm{FGR}}(I)$ and stabilization effect are maximal at I

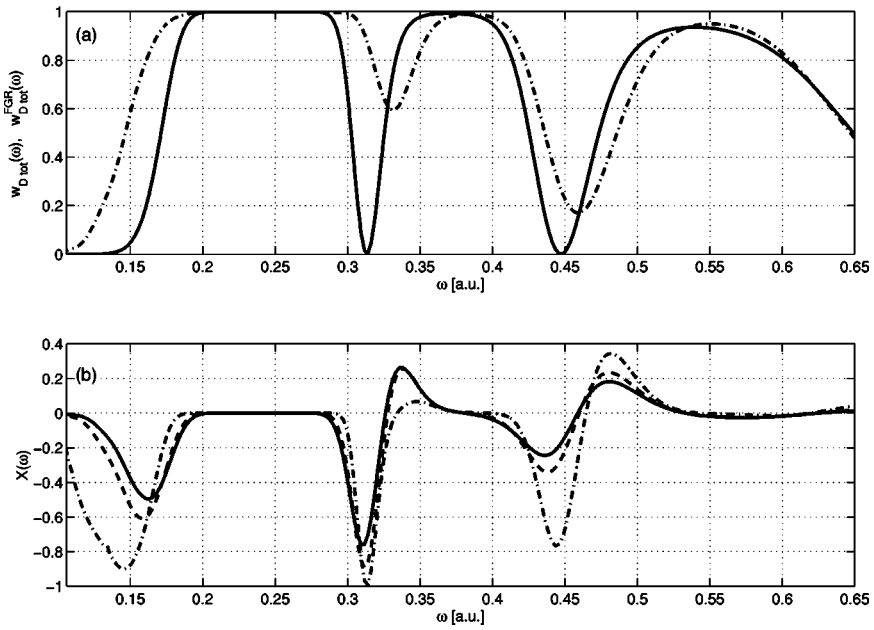

FIG. 8. (a) Exact (dashed line) and Fermi-Golden-Rule (2.9) (solid line) probabilities of dissociation per pulse vs the field frequency ω at $\tau=70$ fs and $I=2\times10^{14}$ W/cm^2. (b) The function $X(I,\omega)\equiv X(\omega)$ (4.1) at different values of the peak light intensity I: solid line, $I=8\times10^{13}$ W/cm^2; dashed line, $I=9\times10^{13}$ W/cm^2; dotted line, $I=10^{14}$ W/cm^2; dash-dotted line, $I=2\times10^{14}$ W/cm^2; $v_0=2$.

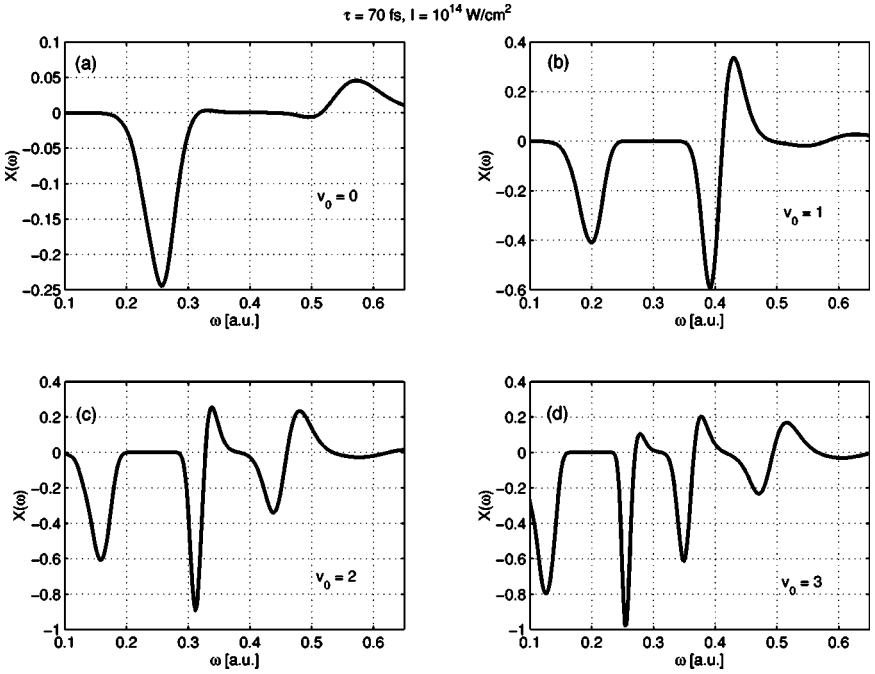

FIG. 9. The function $X(I,\omega) \equiv X(\omega)$ (4.1) at $I=10^{14}$ W/cm^2 and $v_0=0$(a), 1(b), 2(c), 3(d).

$\sim 10^{14}$ W/cm^2. A series of curves $w_{D\,tot}(I)$ in Fig. 7 correspond to the same conditions as in Fig. 6 but with varying pulse duration τ. The effect of stabilization and knee structure are seen to be the more pronounced the shorter is the pulse. It should be emphasized that an origin of the knee structure at the curves $w_{D\,tot}(I)$ in Figs. 6 and 7 is absolutely different from that of the well-known knee structure of the strong-field atomic ionization probability $w_i(I)$ (see, for example, [12]).

A typical example of the frequency dependence of the dissociation probability $w_{D\,tot}(I=\text{const.},\omega)$ is shown by a dashed curve in Fig. 8(a) (calculated at $I=2\times 10^{14}$ W/cm^2, $\tau=70$ fs, and $v_0=2$). The solid curve is the Fermi-Golden-Rule dissociation probability per pulse $w^{\rm FGR}_{D\,tot}(\omega)$ (2.9) calculated at the same values of I,τ, and v_0. Both dependencies are seen to be nonmonotonous, and the regions of saturation ($w_{D\,tot}=1$) are seen to be alternating with regions of rather weak dissociation ($w_{D\,tot}\ll 1$). But the curve $w_{D\,tot}(\omega)$ itself does not give any direct information about stabilization effect and conditions of its realization. Such information can be obtained in the most clear and direct way from the analysis of a difference between $w^{\rm FGR}_{D\,tot}(\omega)$ and $w_{D\,tot}(\omega)$

$$X(\omega)=w^{\rm FGR}_{D\,tot}(I,\omega)-w_{D\,tot}(I,\omega). \tag{4.1}$$

In Fig. 8(b) the function $X(\omega)$ is plotted for several different values of intensity I and for $\tau=70$ fs and $v_0=2$. The regions $X(\omega)>0$ correspond to stabilization and $X(\omega)<0$ — to destabilization of a molecule. In these regions, correspondingly, a strong field decreases or increases the degree of dissociation per pulse compared to $w^{\rm FGR}_{D\,tot}$. Mathemati-

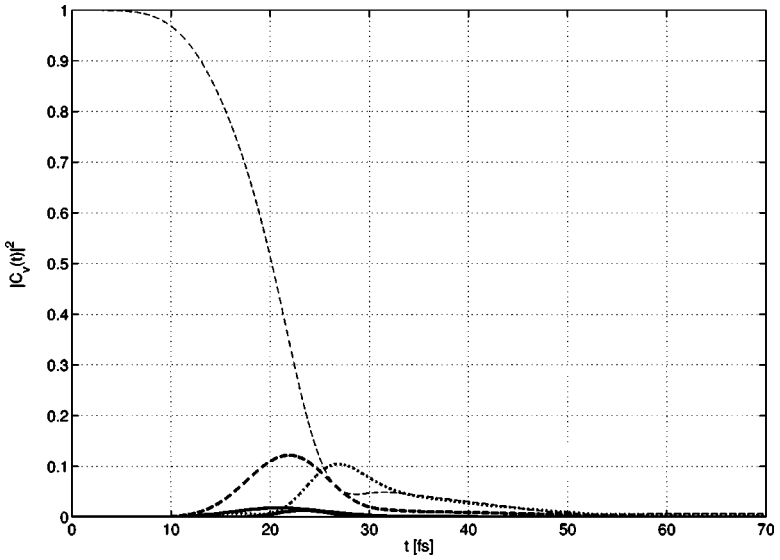

FIG. 10. Time-dependent probabilities to find a molecule at the field-free vibrational levels E_v, $|C_v(t)|^2$ for $I=5\times 10^{14}$ W/cm^2, $\omega=0.338$, $\tau=70$ fs, and $v_0=0$ (solid line), $v=1$ (thick-dashed line), $v=2$ (thin-dashed line), and $v=3$ (dotted line).

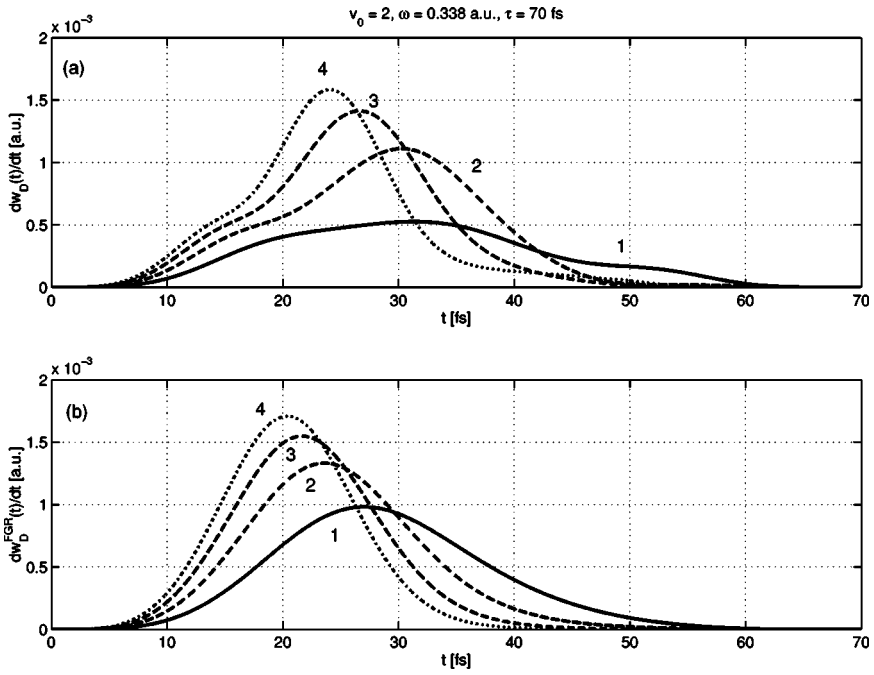

FIG. 11. Exact (a) and Fermi-Golden-Rule (b) rates of dissociation dw_D/dt and dw_D^{FGR}/dt vs time t for the peak light intensity $I=10^{14}$ (1), 2×10^{14} (2), 3×10^{14} (3), and 4×10^{14} (4) W/cm^2.

cally, the reason for both effects consists of a shift of the strong-field curve $w_{D\,tot}(\omega)$ compared to the curve $w_{D\,tot}^{\mathrm{FGR}}(\omega)$, which is clearly seen in Fig. 8(a). For $v_0=2$, the first peak of the curve $X(\omega)$ corresponds to the frequency $\omega\approx0.338$ used in the most of our calculations. At this frequency (for $v_0=2$) the effect of interference stabilization and its manifestations are most pronounced.

Actually, the pictures of Figs. 8 and 9 below give very clear qualitative understanding where and why stabilization or destabilization of a molecule by a strong light field can occur. A structure of the dependence $w_{D\,tot}(\omega)$, an example of which is shown in Fig. 8(a), reflects the structure of the vibrational wave function of the initially populated state φ_{v_0}. In accordance with the Frank-Condon principle, the peaks of $w_{D\,tot}(\omega)$ occur around frequencies which provide a direct ($R=$const.) energy-conserving transition to the unstable electronic state at values of the internuclear distance $R_{antinode}$ corresponding to positions of antinodes of φ_{v_0}:[$\omega=U_1(R_{antinode})-U_0(R_{antinode})-E_{v_0}$]. Oppositely, at frequencies, which provide direct transitions $U_0\rightarrow U_1$ at internuclear distances R_{node} corresponding to positions of nodes of $\varphi_{v_0}[\omega=U_1(R_{node})-U_0(R_{node})-E_{v_0}]$, the function $w_{D\,tot}(\omega)$ has dips. The number of peaks of $w_{D\,tot}(\omega)$ equals

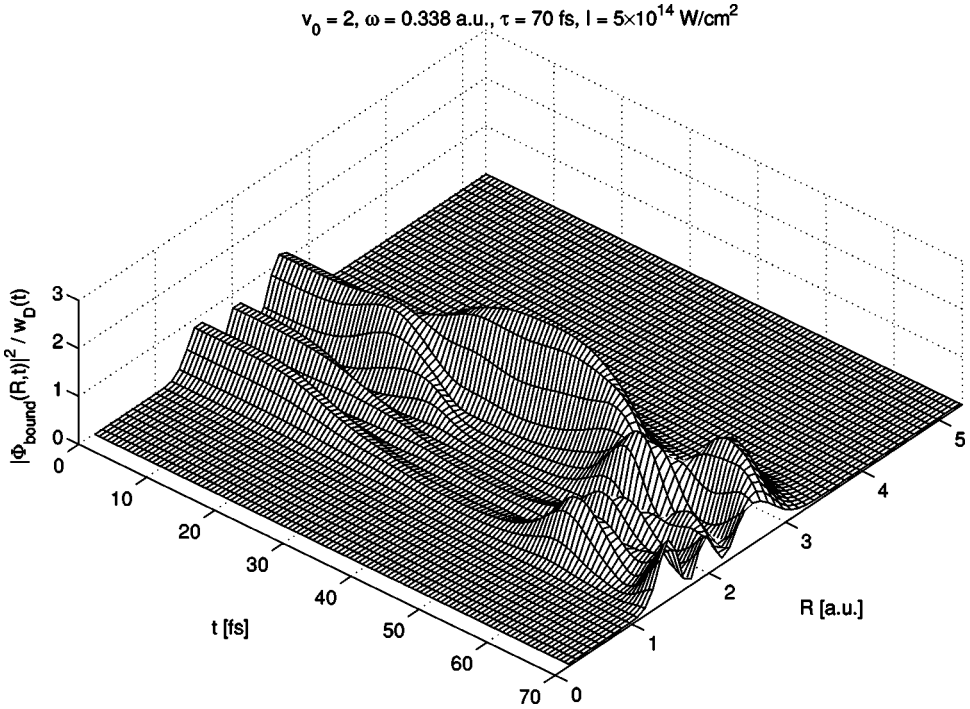

FIG. 12. Evolution in time of the vibrational molecular wave packet arising in the process of photodissociation owing to Raman-type transitions between vibrational levels.

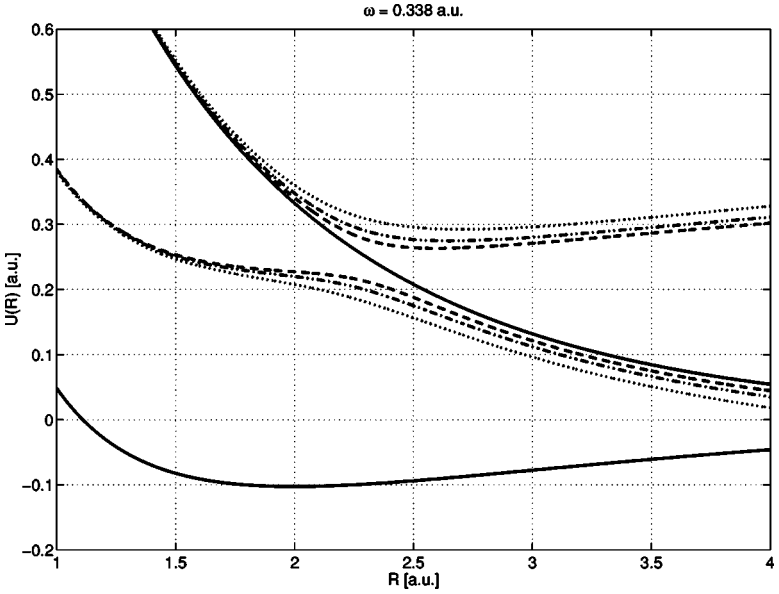

FIG. 13. Field-induced avoided crossing and "adiabatic" potentials curves $U_{\pm}(R)$ for H_2^+ calculated for $I=10^{14}$ W/cm^2 (dashed lines), 2×10^{14} W/cm^2 (dash-dotted lines), and 4×10^{14} W/cm^2 (dotted lines); solid lines are the unperturbed molecular potential curves.

the number of peaks of the function φ_{v_0}. The larger is v_0, the more peaks occur at the curve $w_{D\,tot}(\omega)$. The role of a strong field consists of broadening the curve $w_{D\,tot}(\omega)$ and shifting its dips to the right (to higher-ω regions). For this reason destabilization and stabilization of a molecules ($w_{D\,tot} > w_{D\,tot}^{\mathrm{FGR}}$ and $w_{D\,tot} < w_{D\,tot}^{\mathrm{FGR}}$, correspondingly, occur at falling and rising slopes of dips of the curve $w_{D\,tot}(\omega)$. A number of zones where such following each other's destabilization and stabilization regions can exist coincides with the number of nodes of the initial-state vibrational wave function φ_{v_0}. This conclusion is confirmed directly by the results of calculations shown in Fig. 9 where the function $X(\omega)$ is plotted for a given intensity ($I=10^{14}$ W/cm^2) but for varying values of v_0.

Very interesting and important information about physics of stabilization arises from the analysis of dynamics of photodissociation. The time-dependent probabilities $|C_v(t)|^2$ to find a molecule in the field-free vibrational states φ_v, found from the solution of Eqs. (2.6), are shown in Fig. 10 (for $I=5\times10^{14}$ W/cm^2, $\omega=0.338$, $\tau=70$ fs, and $v_0=2$). The results show that in the process of photodissociation a well-pronounced repopulation of levels E_1 and E_3 takes place. Repopulation of other vibrational levels ($|C_0(t)|^2$ shown in Fig. 10, as well as $|C_v(t)|^2$ with $v=4,5,$etc.) is much less efficient. Time evolution of the probabilities to find a molecule at the most efficiently repopulated levels (E_1,E_2, and E_3) is seen to be rather slow compared to the characteristic localization time $\sim 1,5$ fs of the kernel functions $R_{v,v'}$ (2.5) shown in Fig. 3. This justifies the approximation of semiadiabatic elimination of the continuum used in the transition from Eqs. (2.4) to (2.6).

Time evolution of the exact and Fermi-Golden-Rule rates of photodissociation, dw_D/dt and dw_D^{FGR}/dt, is shown in Fig. 11. In both cases an increase of light intensity makes the peaks of these curves move towards the front wing of the pulse. This shift is explained by saturation: the functions

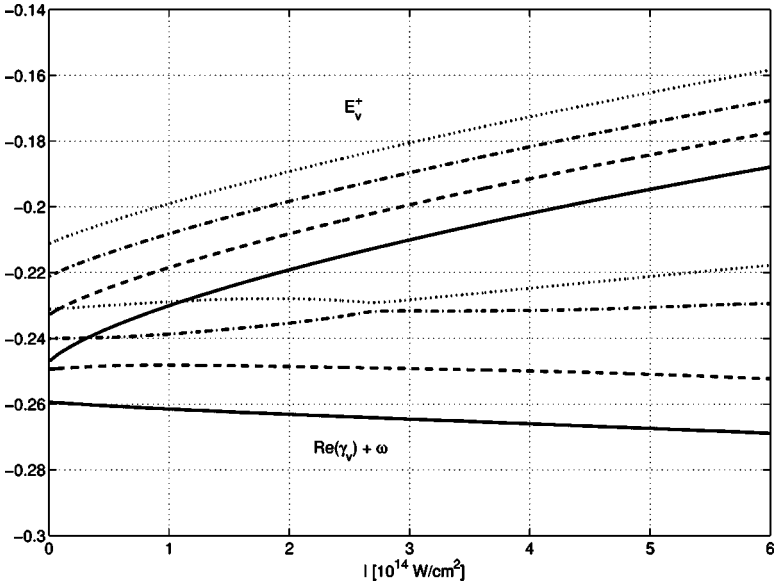

FIG. 14. The functions $\mathrm{Re}(\gamma_v)(I)+\omega$, and $E_v^+(I)$ at $\omega=0.338$ for $v=0$ (solid lines), $v=1$ (dashed lines), $v=2$ (dash-dotted lines), and $v=3$ (dotted lines).

$w_D(t)$ and $w_D^{\mathrm{FGR}}(t)$ approach unity at the lower times, the higher the peak pulse intensity I. Stabilization effect manifests itself in a specific structure of the curves dw_D/dt, arising in a strong field and missing in the case of dw_D^{FGR}/dt: a double twist at the front wing and later position of maxima of the curves $dw_D(t)/dt$ compared to $dw_D^{\mathrm{FGR}}(t)/dt$ at high intensity I.

The calculated time-dependent probability amplitudes $C_v(t)$ were used to investigate evolution of the vibrational wave packet, arising in the process of strong-field photodissociation via repopulation of vibrational levels owing to Raman-type transitions

$$\Phi_{bound}(R,t)=\sum_v C_v(t)\varphi_v(R). \tag{4.2}$$

The structure and dynamics of evolution of this wave packet are described in Fig. 12 (at the same conditions as above, $I=5\times10^{14}$ W/cm^2, $\omega=0.338$, $\tau=70$ fs, and $v_0=2$). For convenience, the wave packet (4.2) is normalized by $w_D(t)=\int_0^\infty dR|\Phi_{bound}(R,t)|^2$. The structure of the wave packet is rather unusual. First, its ''center of mass'' is shifted towards larger R compared to the field-free case. Second, though several vibrational states φ_v with different energies E_v give comparable contribution to $\Phi_{bound}(R,t)$, the wave packet almost does not oscillate during the action of a strong field. Oscillations are suppressed owing to the action of the strong field, which supports the described structure of the wave packet. Only when the field turns off, oscillations arise, because the field becomes too weak to suppress oscillations and support a stable structure of the wave packet.

V. RAMAN-TYPE TRANSITIONS AND THE FIELD-INDUCED AVOIDED CROSSINGS

The method of calculations used above takes into account multiple Raman- or Λ-type transition $E_v\rightarrow E\rightarrow E_{v'}$. This method looks significantly different from that based on the idea of the field-induced avoided crossings though, on the other hand, both methods are aimed to take into account as completely as possible strong-field-induced interaction between levels of bound and unstable electronic states of a molecule. The question is whether these two methods give close or identical results?

The idea of the field-induced avoided crossings in molecules was formulated for the first time in Ref. [8] and later it was used widely in the works on theory of molecule-light interactions and in interpretation of experiments. Briefly, the idea is based on the solution in the two-level approximation of the purely electronic Schrödinger equation with internuclear distance frozen and nuclear kinetic energy dropped from the Hamiltonian. As a result one gets R-dependent field-perturbed electronic energies, which play the role of strong-field ''adiabatic'' potential curves

$$U_\pm(R)=\frac{U_0(R)+\omega+U_1(R)}{2}\pm\left[(U_0(R)+\omega-U_1(R))^2+\frac{d_{01}^2(R)\varepsilon_0^2}{4}\right]^{1/2}. \tag{5.1}$$

For molecular ion H_2^+ these potential curves are described in Fig. 13 for several values of the light intensity I. The upper curves, $U_+(R)$, have minima and, hence, this ''adiabatic'' electronic state gives rise to a strong-field series of vibrational levels. For $v=0,1,2,3$ energies of these levels, E_v^+, are plotted in Fig. 14 in dependence on the light intensity I together with the above-described solutions of the stationary problem for quasienergies (2.11), $\mathrm{Re}(\gamma_v)+\omega$, found by the method of Raman-type transitions. Comparison of these two series of curves shows that the energies E_v^+ differ qualitatively from $\mathrm{Re}(\gamma_v)+\omega$: $E_v^+(I)$ grow proportionally to $\varepsilon_0\sim\sqrt{I}$, whereas $\mathrm{Re}[\gamma_v(I)]+\omega$ change not too regularly and do not experience any systematic growth. In our opinion, this difference indicates a weakness of the field-induced avoided-crossing method. This method exaggerates the role of the two-level Rabi splitting of levels. In the avoided-crossing model, this two-level shift (linear in ε_0) is enforced to all set or strong-field quasienergy vibrational levels. In reality, when a group of levels interacts with a continuum, or with an isolated resonance level, it never shifts altogether, because neighboring levels of the group prevent other levels from a large shift [2]. So, we assume that the quasienergy vibrational spectrum of a molecule in a strong field found by the method of Raman-type transitions is closer to reality than that found by the method of the field-induced avoided crossings. In principle, the difference between two types of spectra shown in Fig. 14 can be seen experimentally by measuring the absorption coefficient of a weak probe field. It should be noted, however, that the functions $\mathrm{Re}[\gamma_v(I)]+\omega$ determine only positions of ''centers of mass'' of quasienergy zones, which experience in reality rather strong broadening, sometimes substituted by narrowing, as it is shown in Fig. 5. It can be rather difficult to get a similar picture by the method of the field-induced avoided crossings with shifts and broadening/narrowing combined together.

It is also reasonable and interesting to compare photodissociation yields calculated by the Raman-type-transitions and avoided-crossing methods. But this is not done yet: for computational problems the calculations by the method of Raman-type transitions were carried out at significantly higher frequencies ω and lower initial vibrational quantum numbers v than the calculations based on the avoided-crossing approach. We hope to perform such a comparison in future and to return to this problem elsewhere.

VI. COMPETITION BETWEEN DISSOCIATION AND MULTIPHOTON IONIZATION

The effects described above are observable (in principle) only if multiphoton ionization does not destroy a molecule in a time shorter than the pulse duration. To specify this condition, we use cross sections of multiphoton ionization calcu-

lated in [13]. The binding energy of an electron in H_2^+ is equal to 1.1 a.u.$\approx$30 eV. At the light frequency $\omega=0.338$ the minimal number of photons necessary for ionization equals four. The cross section σ of four-photon ionization at this frequency is equal approximately to 3×10^{-63} cm^8 W^{-3} (Fig. 3 of Ref. [13]). This corresponds to the rate of ionization (Eq. (40) of Ref. [13])

$$\Gamma=\frac{\sigma I[\mathrm{W/cm^2}]}{\hbar\omega[\mathrm{J}]}\approx 2\times10^{11}\left(\frac{I}{10^{14}}\right)^4. \qquad (6.1)$$

From this estimate we find that at half-height pulse width $\tau_{\text{h-h}}=40$ fs the probability of ionization per pulse $w_i\approx\Gamma\tau<1$ as long as $I<I_{lim}\approx3.3\times10^{14}$ W/cm^2. At intensities not exceeding I_{lim} multiphoton ionization does not destroy a molecule and does not prevent stabilization effects from observation. At shorter pulse durations I_{lim} becomes higher. Besides, inhomogeneity of the field distribution in the focal spot can decrease significantly $\overline{w_i}$ and, hence, increase I_{lim}. Altogether, this makes us think that at $\omega=0.338$ ionization does not destroy a molecule up to intensity about $5/6\times10^{14}$ W/cm^2.

In principle, given estimates can change a little bit because the calculations of Ref. [13] were carried out for equilibrium internuclear distance of a molecule H_2^+, $R=R_e$, whereas in a strong field a molecule can get stretched (as it is seen, e.g., from the picture of Fig. 12). In a stretched molecule cross sections of multiphoton ionization can differ from those of Ref. [13]. At some frquencies and for some initial vibrational states this effect results in a faster ionization [14]. However, this conclusion can strongly depend on a light frequency ω. As far as we know, there were no calculations of the ionization rate in a stretched molecule H_2^+ for $\omega=0.338$ or similarly high frequencies. For this reason, the calculations of Ref. [13] remain the only available source of information for a more or less reasonable conclusion on ionization-dissociation competition under the conditions considered in this paper.

VII. CONCLUSION

To summarize, an approach to a description of strong laser field-molecule interactions is suggested. In this approach multiple Raman-type transitions between vibrational levels of the ground electronic state are taken into account. For a hydrogen molecular ion H_2^+ complex vibrational quasienergies and solutions of the initial-value problem are found. The effect of interference stabilization at vibrational levels is found to occur. The conditions under which the stabilization effect exists are found. Interpretation of the effect is based on the observation of significant coherent repopulation of vibrational levels via Raman-type transitions in the process of photodissociation. Under proper conditions, transitions to the unstable electronic state from these levels interfere with each other and suppress photodissociation. This interpretation is completed by the described effect of narrowing of quasienergy zones in a strong light field. Many manifestations of the stabilization effect are described. In particular, very unusual features of vibrational wave packets created and supported by a strong light field are found to occur.

ACKNOWLEDGMENTS

The work is carried out under partial support of INTAS (Grant No. 99-01495), CRDF (Grant No. RP1-2259), and RFBR (Grant Nos. 99-02-18034 and 00-02-16400).

[1] M.V. Fedorov and A.M. Movsesian, J. Phys. B **21**, L155 (1988).
[2] M. V. Fedorov, *Atomic and Free Electrons in a Strong Light Field* (World Scientific, Singapore, 1991).
[3] J. Hoogenraad, R. Vrijen, and L. Noordam, Phys. Rev. A **50**, 4133 (1994).
[4] A. Giusti-Suzor and F.H. Mies, Phys. Rev. Lett. **68**, 3869 (1992).
[5] E.E. Aubanel, A.D. Bandrauk, and P. Rancourt, Chem. Phys. Lett. **197**, 419 (1992).
[6] E.E. Aubanel, J.-M. Gautier, and A.D. Bandrauk, Phys. Rev. A **48**, 2145 (1993).
[7] A. D. Bandrauk, *Molecules in Intense Laser Fields* (Academic Press, New York, 1995).
[8] M.V. Fedorov, O.V. Kudrevatova, A.A. Samokhin, and V.P. Makarov, Opt. Commun. **13**, 299 (1975).
[9] D.R. Bates, K. Ledsham, and A.L. Stewart, Philos. Trans. R. Soc. London, Ser. A **A246**, 215 (1953).
[10] S. Cohen, D.L. Judd, and R.J. Riddell, Phys. Rev. **119**, 384 (1960).
[11] L. D. Landau and E. M. Lifshitz, *Quantum Mechanics* (Pergamon Press, New York, 1977).
[12] D. Bauer and F. Ceccherini, Opt. Express **8**, 377 (2001).
[13] Moon-Gu Baik, M. Pont, and R. Shakeshaft, Phys. Rev. A **54**, 1570 (1996).
[14] S. Chelkowski, T. Zuo, O. Atabek, and A.D. Bandrauk, Phys. Rev. A **46**, R5342 (1992).